AGU PUBLICATIONS

Geophysical Research Letters

RESEARCH LETTER
10.1002/2015GL067267

Key Points:
- Winter cyclones are projected to decrease on the Australian east coast
- Cyclones associated with heavy rainfall may increase in frequency
- Projections of warm season cyclones remain uncertain

Supporting Information:
- Figures S1–S5 caption and Table S1
- Figure S1
- Figure S2
- Figure S3
- Figure S4
- Figure S5

Correspondence to:
A. S. Pepler,
a.pepler@student.unsw.edu.au

Citation:
Pepler, A. S., A. Di Luca, F. Ji, L. V. Alexander, J. P. Evans, and S. C. Sherwood (2016), Projected changes in east Australian midlatitude cyclones during the 21st century, *Geophys. Res. Lett.*, *43*, doi:10.1002/2015GL067267.

Received 1 DEC 2015
Accepted 13 DEC 2015
Accepted article online 16 DEC 2015

Projected changes in east Australian midlatitude cyclones during the 21st century

Acacia S. Pepler[1], Alejandro Di Luca[1], Fei Ji[2], Lisa V. Alexander[1], Jason P. Evans[1], and Steven C. Sherwood[1]

[1]Centre for Excellence for Climate System Science and Climate Change Research Centre, University of New South Wales, Kensington, New South Wales, Australia, [2]New South Wales Office of Environment and Heritage, Sydney, New South Wales, Australia

Abstract The east coast of Australia is regularly influenced by midlatitude cyclones known as East Coast Lows. These form in a range of synoptic situations and are both a cause of severe weather and an important contributor to water security. This paper presents the first projections of future cyclone activity in this region using a regional climate model ensemble, with the use of a range of cyclone identification methods increasing the robustness of results. While there is considerable uncertainty in projections of cyclone frequency during the warm months, there is a robust agreement on a decreased frequency of cyclones during the winter months, when they are most common in the current climate. However, there is a potential increase in the frequency of cyclones with heavy rainfall and those closest to the coast and accordingly those with potential for severe flooding.

1. Introduction

The midlatitude cyclones known as East Coast Lows (ECLs) are one of the most important features of the climate of Australia's east coast. They are responsible for the majority of major floods [*Callaghan and Power*, 2014] and large waves [*Dowdy et al*., 2014] in the region and are critically important to both annual rainfall totals and water security [*Pepler and Rakich*, 2010]. For this reason, there is substantial interest in how the frequency, intensity, or characteristics of these systems may change over the coming century.

ECL is a broad and poorly defined term and can include systems as varied as cut-off lows, extropical cyclones, and lows that develop in situ from a coastal surface trough [e.g., *Speer et al*., 2009], many of which satisfy the *Sanders and Gyakum* [1980] "bomb" criterion. Accordingly, their spatial scales range from as small as 200 km to over 1000 km, and temporal scales range from less than a day to several days.

While the skill of global climate models (GCMs) at simulating cyclones continues to improve, their low spatial resolutions tend to result in small-scale cyclones and associated severe weather being either absent or poorly simulated [e.g., *Wehner et al*., 2015]. Consequently, while a projected southward shift in the midlatitude storm tracks over the coming century is a robust result across GCMs [*Bengtsson et al*., 2006; *Chang et al*., 2012; *Grieger et al*., 2014], this may not accurately reflect changes in the full range of systems, particularly those of smaller spatial or temporal scales.

In Australia, several studies have attempted to assess ECL projections in GCMs [*Dowdy et al*., 2013, 2014] or RCMs [*Ji et al*., 2015] by investigating changes in an upper level diagnostic that favors the formation of ECLs, rather than identifying individual ECL events. In line with previous research, these studies identified a consistent decline in future ECL activity, with declines in the average annual frequency of 15–40% by 2100. Trends were strongest during the cool season and for events of moderate intensity. However, the nature of this method does not allow detailed assessment of changes in the location, characteristics, or impacts of individual ECLs, preventing a full analysis of these changes. Furthermore, the method may fail to identify the full range of systems, particularly small-scale lows and those events that develop during the summer months [*Pepler et al*., 2015].

This paper builds on the studies of *Dowdy et al*. [2013, 2014] and *Ji et al*. [2015] to present the most robust assessment of future ECL activity currently available. We use a Regional Climate Model (RCM) ensemble that has been designed to incorporate the full range of projections across southeastern Australia, while maintaining high independence of errors and skill at representing the current southeast Australian climate [*Evans et al*., 2014a]. As different automated methods used to identify and track cyclones have different error

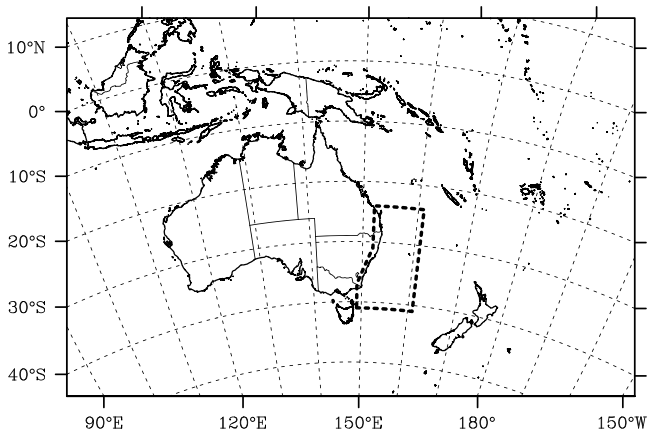

Figure 1. The 50 km resolution NARCliM model domain, with the ECL identification region indicated by a thick dashed line.

patterns when representing observed ECL activity [*Pepler et al*., 2015] and projections of cyclone activity in the Northern Hemisphere vary somewhat between methods [*Ulbrich et al*., 2013], we present results using several methods of identifying ECLs. This allows a more detailed assessment of the full uncertainties associated with future changes in ECLs.

2. Data and Methods

2.1. The NARCliM Regional Climate Model Ensemble

The New South Wales/Australian Capital Territory Regional Climate Model (NARCliM) ensemble has been extensively described in *Evans et al*. [2014a]. This is a 12 member RCM ensemble of projections for Australia, designed with a particular focus on the southeast coast. Four CMIP3 GCMs, in addition to the National Centers for Environmental Prediction (NCEP)-National Center for Atmospheric Research (NCAR) Reanalysis [*Kalnay et al*., 1996], were downscaled using version 3.3 of the Weather Research and Forecasting (WRF) model to a 50 km resolution for a region that extends well beyond the Australian mainland (CORDEX-Australasia; Figure 1). Three periods were used (1990–2009, 2020–2039, and 2060–2079), with future projections based on a high-emissions scenario (A2); only the 50 km resolution runs for the present and far-future (2060–2079) periods are used for this study.

The four CMIP3 models used are CCCMA3.1, ECHAM5, MIROC3.2, and CSIRO-Mk3.0. These were selected based on model performance over Australia, independence of errors, and to span the full range of potential future climates over southeastern Australia. The three WRF RCMs were also chosen for adequate skill and error independence, following a comprehensive analysis of 36 different combinations of physics parametrizations over eight significant ECLs [*Evans et al*., 2012; *Ji et al*., 2014]. The resultant ensemble improves substantially on the GCMs in the simulation of Australian mean and extreme rainfall [*Evans et al*., 2013, 2014b].

2.2. The ECL Identification Method Ensemble

Due to the sensitivity of classifying ECLs according to the method used to identify cyclones [*Neu et al*., 2013; *Pepler et al*., 2015], three different ECL identification methods are used for this paper. These are described in more detail in *Pepler et al*. [2015], but all show high skill in identifying ECLs associated with large weather impacts, while exhibiting different seasonal patterns and interannual variability. Notably, the method with the highest skill score varied between ECLs that developed in different synoptic situations, with a range of ECL identification methods recommended to robustly assess variability or changes. While the NARCliM data set is available at a 3-hourly resolution only the 6-hourly pressure grids are used for this paper, for consistency with how the same methods have been applied to reanalyses.

The first method is based on *Dowdy et al*. [2013] and has previously been applied to the NARCliM data set by *Ji et al*. [2015]. Rather than identifying individual cyclones, it identifies periods of anomalously high upper level (500 hPa) geostrophic vorticity (ULGV) as an indicator of an increased risk of ECL activity. In addition, we use two methods that directly identify and track ECLs from the gridded mean sea level pressure (MSLP) data, providing additional information such as ECL intensity, location, and duration. These methods have been applied to both the raw 50 km resolution MSLP fields, as well as MSLP that has been regridded to the same 150 km resolution as used in *Pepler et al*. [2015]. This allows us to test the sensitivity of projections to the grid resolution used, which has been noted as an influence on projections of low pressure systems in *Wehner et al*. [2015], with the coarser-resolution data less sensitive to small-scale features and potentially identifying a different subset of lows.

The pressure gradient (PG) method is based on *Browning and Goodwin* [2013] as adapted by *Di Luca et al*. [2015] and uses local MSLP gradients to identify a low pressure system with a closed contour. The intensity

of a low is given by the average pressure gradient for a 200 km radius around the low center, although several other measures are available. The Laplacian (LAP) method is derived from *Murray and Simmonds* [1991] and *Simmonds et al*. [1999], and identifies low pressure systems as a maxima of the Laplacian of MSLP, before identifying an associated closed low. The intensity of a low is given by the average of the laplacian for a 200 km radius around the center. Both of these methods then collate individual lows into cyclone tracks, with an ECL event identified where a track persists for at least 6 h and crosses through the ECL domain in Figure 1.

The intensity of low pressure systems is highly dependent on data set resolution [*Di Luca et al*., 2015], while the number of low pressure systems identified for a given intensity threshold can vary substantially between models. As any automated tracking scheme intrinsically requires a minimum intensity threshold to identify a low, for this paper we select an intensity threshold for each method and model, such that each data set has the same frequency of ECLs in the current period (Table S1 in the supporting information). This is consistent with similar studies [*Dowdy et al*., 2013; *Ji et al*., 2015] and enables an easier comparison between models and methods. While we primarily use a threshold that gives a frequency of 22 ECLs per year for each member, consistent with an observed data set [*Speer et al*., 2009], using a constant threshold across all 12 models that gives the same average ECL frequency results in the same overall projections (Figure S1).

For the purposes of assessing ECLs associated with severe weather, an ECL is considered to have heavy rain when the average 6-hourly rainfall accumulation within 500 km of the low center exceeds 6 mm for at least one instance. This is equivalent to a daily rainfall total of 24 mm, similar to the threshold of significant rain used in the *Speer et al*. [2009] database (25 mm). An alternate metric of heavy rain is where any point within 500 km of the low center has a 6-hourly rainfall accumulation exceeding 50 mm, an arbitrary threshold that is observed for a similar proportion of ECLs (~8 p.a.). An ECL is considered to have strong winds where the mean hourly wind speed within 500 km of the low center exceeds 50 km/h in at least one instance, equivalent to the Bureau of Meteorology's "strong wind" threshold and the "moderate gale" threshold on the Beaufort wind scale. While the number of ECLs with severe weather varies substantially between models and seasons, these thresholds were chosen to ensure that every combination has at least five severe events during the current climate for each season.

3. Skill of the NARCliM Ensemble at Simulating Present ECL Activity

While the parametrizations used for the WRF downscaling have skill at simulating observed ECL case studies [*Evans et al*., 2012], there are large uncertainties in both ECL frequency and characteristics when assessed across a range of high-resolution reanalysis products [*Di Luca et al*., 2015]. Consequently, it is difficult to determine a "truth" for assessing high-resolution RCMs, particularly when using a model-dependent intensity threshold.

The NARCliM ensemble reproduces the interannual variability of ECL activity well. Across all models and methods, the average standard deviation was 4.8, ranging between 3.4 and 7.7 for individual models. In comparison, the manual *Speer et al*. [2009] database had an annual standard deviation of 4.4, with annual ECL frequency ranging between 13 in 2006 and 32 in 1976.

In contrast, the seasonality of ECL activity is poorly simulated when RCM simulations are driven by GCMs. *Speer et al*. [2009] identified 57% of ECLs during the cool season (May–October), increasing to 74% of ECLs that undergo "explosive" intensification. Where the RCM has boundary conditions provided by the NCEP reanalysis, all RCMs and methods also have 55–60% of ECLs during the May–October period, consistent with observed data sets.

When the RCMs use boundary conditions from the CMIP3 ensemble, only 40–50% of ECLs identified by the LAP method occur during the cool season, and 30–40% of ECLs using the PG method, consistent across both spatial resolutions. This is also a feature of ECLs identified directly from the GCMs where 6-hourly MSLP is available (CCCMA3.1 and ECHAM5) and may be related to systematic biases in the representation of broadscale features such as the subtropical ridge [*Grose et al*., 2015]. Interestingly, the seasonal distribution of ECLs using the ULGV method is similar between the NCEP- and GCM-driven members, reflecting a strong seasonality of mean ULGV in both reanalyses and climate models.

For the remainder of this paper, results will be separated into the cool (May–October) and warm (November–April) seasons, to counter the impact that shifted seasonality may have on changes in annual ECL frequency.

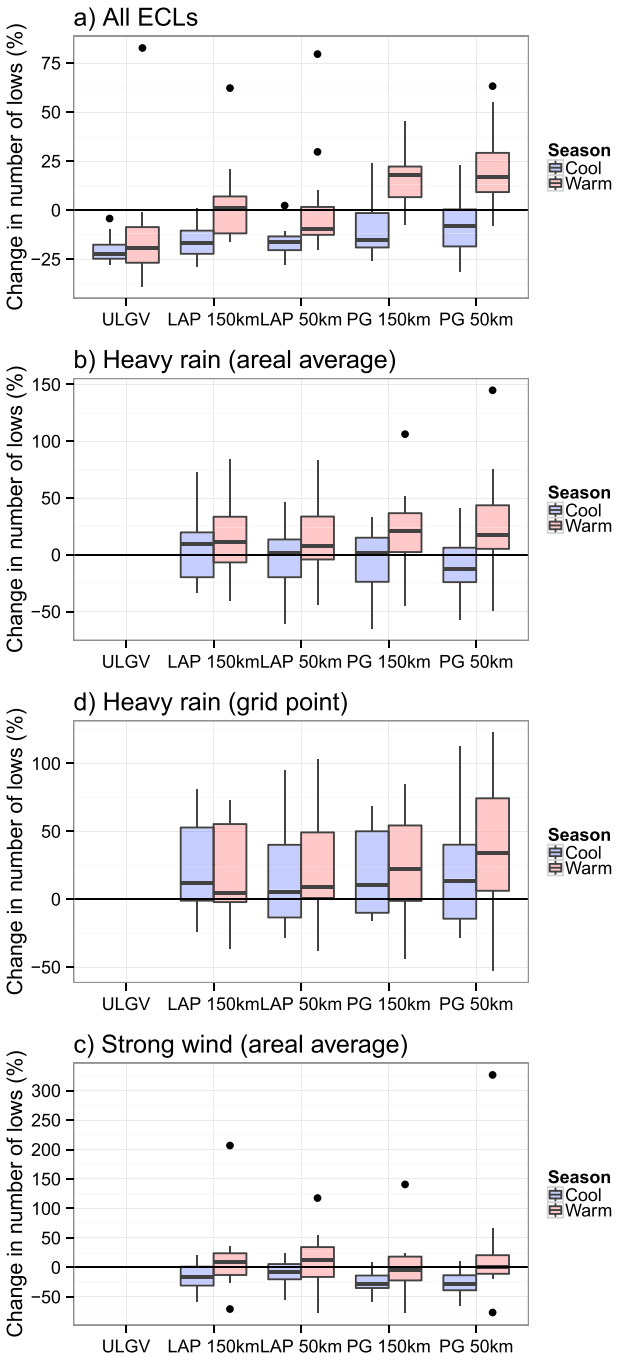

Figure 2. (a) Percentage change in the total number of ECLs per year between 1990–2009 and 2060–2079; (b) Percentage change in the number of ECLs where the mean rainfall intensity within 500 km of the low center exceeds 6 mm/6 h in at least one instance; (c) Percentage change in the number of ECLs where the mean hourly wind speed within 500 km of the low center exceeds 50 km/h in at least one instance; and (d) Percentage change in the number of ECLs where the maximum rainfall intensity within 500 km of the low center exceeds 50 mm/6 h in at least one instance. In all cases ECLs are selected using a model-dependent threshold that gives 22 ECLs per year in the current climate, with trends shown for the cool season (May–October) and warm season (November–April) separately.

4. ECL Projections

Figure 2a shows the range of ECL projections across the full ensemble, segregated by season, where an intensity threshold is used that identifies 22 ECLs per year in the current climate. Where applicable, resulting trends are tested at the 5% significance level using a students *t* test.

There is no consistent change projected in the frequency of warm season ECLs by the late 21st century, with a median change of just 0.5% and projections ranging from −40% to +85%. In contrast, a clear and robust decline is projected for the cool season, with 83% of combinations projecting a decline in ECL frequency, of which 37% are statistically significant. The median decline is 16.7% or 0.49 standard deviations. Declines are strongest for the ULGV method, with smallest changes using the PG method and the MIROC-R3 simulation.

The results are insensitive to the specific parameters used in individual tracking schemes, with very similar projections for the LAP method when lows were instead restricted using the intensity over a 500 km radius or with events restricted to those persisting for more than 24 h (Figure S2). The results are also relatively insensitive to the precise intensity threshold used, although larger median declines of 28% are projected for cool season when using a higher intensity threshold that gives 5 ECLs per year (Figure S3). This is in contrast to results for *Ji et al.* [2015], who found strongest declines were projected for medium-intensity ECLs.

In the current climate, 1–2 ECLs per year are associated with significant impacts [*Callaghan and Power*, 2014; *Hopkins and Holland*, 1997]. The most notable and memorable events have occurred approximately once per decade, such as during June 2007 [*Chambers et al.*, 2014] or more recently in April 2015. It is difficult to

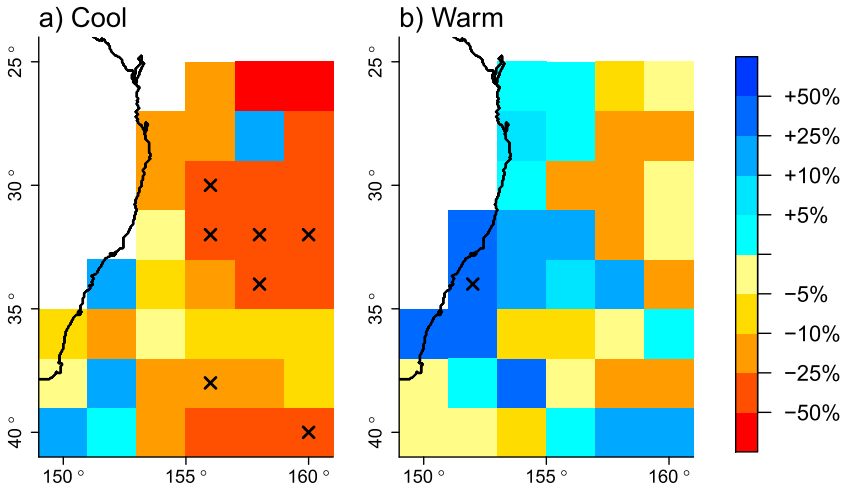

Figure 3. Median percentage change in ECL frequency between 1990–2009 and 2060–2079, across 12 RCMs and four methods for (a) May–October and (b) November–April. The intensity threshold used for each method/model is the same threshold that gives 22 ECLs per year, as used in Figure 2. Crosses indicate areas where at least 75% of members indicate the same direction of change.

assess trends in these most intense events, given the high interannual and decadal variability in ECLs during both the present and future periods. However, when selecting the 20 strongest ECLs during each period for each method, only 18% of model combinations have a statistically significant change in intensity, while 68% of combinations have at least one ECL in the 2060–2079 period that has a higher maximum intensity than produced by the same model and method in the 1990–2009 period.

For those identification methods where ECL location information is available (LAP and PG), we can also assess changes in the frequency of ECLs associated with extreme weather around the low center. Despite the clear decrease in the frequency of cool season ECLs, the majority of models and methods project no change in the frequency of ECLs associated with heavy rain (Figure 2b), and an increase in the frequency of ECLs where the maximum 6-hourly rainfall accumulation at any point exceeds 50 mm (Figure 2c). This reflects an increase in the average maximum rainfall associated with a given ECL, particularly for the LAP method (Figure S4) and is consistent with projections for similar systems such as tropical cyclones [e.g., *Knutson et al.*, 2013]. In comparison, there is large uncertainty in projections of ECLs with strong winds, although a decline in cool season strong wind events is projected using the PG method (Figure 2d). As with projections for total ECL activity, changes are not statistically significant for the majority of methods given the high interannual variability; however, the consistency in results across a variety of GCMs, RCMs, and detection methods adds robustness to the results.

Previous studies have noted substantial spatial variation in projections of cyclone activity [*Colle et al.*, 2013; *Ulbrich et al.*, 2013]; consequently, it is important to know the spatial patterns of changes. For those methods where ECL location information is available (LAP and PG) the cool season decrease is strongest in the northern half of the ECL domain, particularly for the LAP method, consistent with projections of a southward shift in the storm tracks (Figure 3a). While these changes are generally not statistically significant given the high interannual variability, more than 75% of models project a decline in ECL activity in much of the northeastern part of the region. Projections are less consistent for the area directly off the east coast than farther offshore, similar to results in *Colle et al.* [2013], suggesting a higher level of uncertainty for the area where changes in ECL activity have the largest human impact.

Consistent with Figure 2, there is no clear trend in ECL frequency across most of the domain during the warm season (Figure 3b). Median changes are generally positive along the east coast, with part of the south coast experiencing increases in ECL frequency in more than 75% of combinations, including just south of the major city of Sydney (33°S).

The longitudinal variation in projections is most pronounced for the PG method (Figure S5). When we restrict analysis to the subset of ECLs that pass within 500 km of the coast, projections using the LAP method remain

consistent with those for all ECLs in both seasons. In contrast, there is a marked strengthening in warm season projections using the PG method, with the median projected change increasing from +17% to +29%, while the median projected change in cool season ECLs is close to zero. This adds additional uncertainty for projections of the ECLs with the greatest impacts on the east coast.

5. Conclusions

This paper presents the most robust assessment to date of projections of midlatitude cyclones off the east coast of Australia, using an ensemble of regional climate models as well as a range of methods of identifying cyclones. There is a large range in projections between methods, similar to or larger than the uncertainty related to the RCM ensemble, and substantially larger than the uncertainty related to the parameter choice for a given method (Figures S1–S3). This is an important result and reaffirms the need for studies to apply a range of cyclone detection methods when assessing future projections. The MIROC-R3 simulation projected an anomalously large increase in the frequency of warm season ECLs and associated severe weather relative to other RCMs, which is worthy of further investigation.

There is no clear trend in the total number of ECLs during the warm months November–April, with projections particularly sensitive to ECL definitions during this season. This may be because warm season ECLs are typically smaller and less intense, with much larger variations between methods in successfully identifying ECLs in this season [*Di Luca et al*., 2015; *Pepler et al*., 2015]. However, an increased frequency is projected along the Australian east coast in the majority of models, particularly in the southeast and for the PG method. This may be related to the projected intensification of the East Australian Current and associated sea surface temperature (SST) extremes, which has one of the fastest rates of warming in the world [*Oliver et al*., 2013], with warmer SSTs and stronger eddies potentially enhancing ECL-related severe rainfall [*Chambers et al*., 2014].

In contrast, there is a consistent and robust decreasing trend in the frequency of cool season ECLs, with an average decline of 16.7%. This is consistent with previous studies such as *Dowdy et al*. [2013], as well as projections of a southward shift in midlatitude cyclones [*Bengtsson et al*., 2006] over the coming century. These trends are strongest in the eastern part of the domain, with weaker trends projected for areas immediately along the east coast. This is most apparent using the PG method (Figure S5), which is also the method most sensitive to small scale and summer ECLs [*Pepler et al*., 2015]. These results suggest the impact of projected declines on the east coast could be smaller than projections of total ECL frequency may suggest [e.g., *Dowdy et al*., 2013]. However, it is important to note that the NARCliM RCM ensemble and the driving GCMs underestimate the frequency of cool season ECLs under the current climate, particularly for the PG method and near the coast, so may be unable to simulate all types of ECLs.

While the 20 year timespans in the NARCliM ensemble make it difficult to assess changes in the most intense systems, little change is observed in the intensities of the 20 strongest ECLs per year. While changes are not statistically significant, owing to the large interannual variability and small sample sizes, results suggest no change or an increase in the frequency of ECLs associated with heavy rainfall in all seasons. In contrast, there is large uncertainty but a possible decline in ECLs associated with strong winds, suggesting very different factors are at play for different types of impacts. When combined with the weaker declines in frequency projected for ECLs closer to the coast, this could result in increases in the frequency of severe weather and coastal flooding regardless of changes in overall rain totals and is a critical area for further research.

Acknowledgments

This research was supported by the Australian Research Council Centre of Excellence for Climate System Science grant CE110001028 and Linkage project grant LP120200777. Jason Evans was supported by the Australian Research Council Future Fellowship FT110100576, with the WRF downscaled runs available thanks to the NSW Office of Environment and Heritage backed NSW/ACT Regional Climate Modelling (NARCliM) Project and the Eastern Seaboard Climate Change Initiative—East Coast Low Project (ESCCI-ECL). This research was undertaken with the assistance of resources provided at the NCI National Facility systems at the Australian National University through the National Computational Merit Allocation Scheme supported by the Australian Government. NARCliM data can be obtained freely from the Adapt NSW webpage (http://www.climatechange.environment.nsw.gov.au/Climate-projections-for-NSW/Download-datasets), while the derived East Coast Low data sets can be obtained upon request from Fei Ji (ULGV method; Fei.Ji@environment.nsw.gov.au), Alejandro Di Luca (PG method; a.diluca@unsw.edu.au), and Acacia Pepler (LAP method, a.pepler@student.unsw.edu.au).

References

Bengtsson, L., K. I. Hodges, and E. Roeckner (2006), Storm tracks and climate change, *J. Clim.*, *19*(15), 3518–3543, doi:10.1175/JCLI3815.1.

Browning, S. A., and I. D. Goodwin (2013), Large-scale influences on the evolution of winter subtropical maritime cyclones affecting Australia's east coast, *Mon. Weather Rev.*, *141*(7), 2416–2431, doi:10.1175/MWR-D-12-00312.1.

Callaghan, J., and S. B. Power (2014), Major coastal flooding in southeastern Australia 1860–2012, associated deaths and weather systems, *Aust. Meteorol. Oceanogr. J.*, *64*, 183–213.

Chambers, C. R. S., G. B. Brassington, I. Simmonds, and K. Walsh (2014), Precipitation changes due to the introduction of eddy-resolved sea surface temperatures into simulations of the 'Pasha Bulker' Australian east coast low of June 2007, *Meteorol. Atmos. Phys.*, *125*, 1–15.

Chang, E. K. M., Y. Guo, and X. Xia (2012), CMIP5 multimodel ensemble projection of storm track change under global warming, *J. Geophys. Res.*, *117*, D23118, doi:10.1029/2012JD018578.

Colle, B. A., Z. Zhang, K. A. Lombardo, E. Chang, P. Liu, and M. Zhang (2013), Historical evaluation and future prediction of eastern North America and western Atlantic extratropical cyclones in the CMIP5 models during the cool season, *J. Clim.*, *26*, 6882–6903, doi:10.1175/JCLI-D-12-00498.1.

Di Luca, A., J. P. Evans, A. S. Pepler, L. Alexander, and D. Argüeso (2015), Resolution sensitivity of cyclone climatology over eastern Australia using six reanalysis products, *J. Clim.*, doi:10.1175/JCLI-D-14-00645.1.

Dowdy, A. J., G. A. Mills, B. Timbal, and Y. Wang (2013), Changes in the risk of extratropical cyclones in eastern Australia, *J. Clim.*, *26*(4), 1403–1417, doi:10.1175/JCLI-D-12-00192.1.

Dowdy, A. J., G. A. Mills, B. Timbal, and Y. Wang (2014), Fewer large waves projected for eastern Australia due to decreasing storminess, *Nat. Clim. Change*, *4*, 283–286, doi:10.1038/nclimate2142.

Evans, J. P., M. Ekström, and F. Ji (2012), Evaluating the performance of a WRF physics ensemble over South-East Australia, *Clim. Dyn.*, *39*(6), 1241–1258, doi:10.1007/s00382-011-1244-5.

Evans, J. P., L. Fita, D. Argüeso, and Y. Liu (2013), Initial NARCliM evaluation, in *MODSIM2013, 20th International Congress on Modelling and Simulation*, edited by J. Piantadosi, R. S. Anderssen, and J. Boland, pp. 2765–2771, Modelling and Simulation Society of Australia and New Zealand Inc., Adelaide, Australia.

Evans, J. P., F. Ji, C. Lee, P. Smith, D. Argüeso, and L. Fita (2014a), Design of a regional climate modelling projection ensemble experiment—NARCliM, *Geosci. Model Dev.*, *7*(2), 621–629, doi:10.5194/gmd-7-621-2014.

Evans, J. P., D. Argüeso, R. Olson, and A. Di Luca (2014b), NARCliM extreme precipitation indices report NARCliM Tech. Note 6, 109 pp., NARCliM Consortium, Sydney, Australia.

Grieger, J., G. C. Leckebusch, M. G. Donat, M. Schuster, and U. Ulbrich (2014), Southern Hemisphere winter cyclone activity under recent and future climate conditions in multi-model AOGCM simulations, *Int. J. Climatol.*, *34*(12), 3400–3416, doi:10.1002/joc.3917.

Grose, M. R., B. Timbal, L. Wilson, J. Bathols, and D. Kent (2015), The subtropical ridge in CMIP5 models, and implications for projections of rainfall in southeast Australia, *Aust. Meteorol. Oceanogr. J.*, *65*, 90–106.

Hopkins, L. C., and G. J. Holland (1997), Australian heavy-rain days and associated east coast cyclones: 1958–92, *J. Clim.*, *10*(4), 621–635.

Ji, F., M. Ekström, J. P. Evans, and J. Teng (2014), Evaluating rainfall patterns using physics scheme ensembles from a regional atmospheric model, *Theor. Appl. Climatol.*, *115*(1–2), 297–304, doi:10.1007/s00704-013-0904-2.

Ji, F., J. P. Evans, D. Argüeso, L. Fita, and A. Di Luca (2015), Using large-scale diagnostic quantities to investigate change in East Coast Lows, *Clim. Dyn.*, 1–11, doi:10.1007/s00382-015-2481-9.

Kalnay, E., et al. (1996), The NCEP/NCAR 40-year reanalysis project, *Bull. Am. Meteorol. Soc.*, *77*(3), 437–471, doi:10.1175/1520-0477(1996)077<0437:TNYRP>2.0.CO;2.

Knutson, T. R., J. J. Sirutis, G. A. Vecchi, S. Garner, M. Zhao, H.-S. Kim, M. Bender, R. E. Tuleya, I. M. Held, and G. Villarini (2013), Dynamical downscaling projections of twenty-first-century Atlantic hurricane activity: CMIP3 and CMIP5 model-based scenarios, *J. Clim.*, *26*(17), 6591–6617, doi:10.1175/JCLI-D-12-00539.1.

Murray, R. J., and I. Simmonds (1991), A numerical scheme for tracking cyclone centres from digital data. Part I: Development and operation of the scheme, *Aust. Meteorol. Mag.*, *39*(3), 155–166.

Neu, U., et al. (2013), IMILAST: A community effort to intercompare extratropical cyclone detection and tracking algorithms, *Bull. Am. Meteorol. Soc.*, *94*(4), 529–547, doi:10.1175/BAMS-D-11-00154.1.

Oliver, E. C. J., S. J. Wotherspoon, M. A. Chamberlain, and N. J. Holbrook (2013), Projected Tasman Sea extremes in sea surface temperature through the 21st Century, *J. Clim.*, *27*, 1980–1998, doi:10.1175/JCLI-D-13-00259.1.

Pepler, A. S., and C. S. Rakich (2010), Extreme inflow events and synoptic forcing in Sydney catchments, *IOP Conf. Ser.: Earth Environ. Sci.*, *11*, 012010, doi:10.1088/1755-1315/11/1/012010.

Pepler, A. S., A. Di Luca, F. Ji, L. V. Alexander, J. P. Evans, and S. C. Sherwood (2015), Impact of identification method on the inferred characteristics and variability of Australian East Coast Lows, *Mon. Weather Rev.*, *143*(3), 864–877, doi:10.1175/MWR-D-14-00188.1.

Sanders, F., and J. R. Gyakum (1980), Synoptic-dynamic climatology of the 'bomb', *Mon. Weather Rev.*, *108*(10), 1589–1606, doi:10.1175/1520-0493(1980)108<1589:SDCOT>2.0.CO;2.

Simmonds, I., R. J. Murray, and R. M. Leighton (1999), A refinement of cyclone tracking methods with data from FROST, *Aust. Meteorol. Mag.*, 35–49.

Speer, M. S., P. Wiles, and A. Pepler (2009), Low pressure systems off the New South Wales coast and associated hazardous weather: Establishment of a database, *Aust. Meteorol. Oceanogr. J.*, *58*(1), 29–39.

Ulbrich, U., et al. (2013), Are Greenhouse Gas Signals of Northern Hemisphere winter extra-tropical cyclone activity dependent on the identification and tracking algorithm?, *Meteorol. Z.*, *22*(1), 61–68, doi:10.1127/0941-2948/2013/0420.

Wehner, W. M., Prabhat, K. A. Reed, D. Stone, W. D. Collins, and J. Bacmeister (2015), Resolution dependence of future tropical cyclone projections of CAM5.1 in the U.S. CLIVAR Hurricane Working Group idealized configurations, *J. Clim.*, *28*(10), 3905–3925, doi:10.1175/JCLI-D-14-00311.1.